Supplement of Atmos. Chem. Phys., 19, 14031–14056, 2019
https://doi.org/10.5194/acp-19-14031-2019-supplement

Atmospheric Chemistry and Physics
Open Access
EGU

Supplement of

Is the recovery of stratospheric O_3 speeding up in the Southern Hemisphere? An evaluation from the first IASI decadal record (2008–2017)

Catherine Wespes et al.

Correspondence to: Catherine Wespes (cwespes@ulb.ac.be)

Contents of this file

1 Figure S1

Figure S1 displays the latitudinal distribution of MUSt O_3 columns as a function of time observed from IASI in comparison with that simulated by the BASCOE CTM with its standard chemical mechanism (smoothed by the IASI averaging kernels), as well as the IASI-BASCOE differences for the MUSt and the LSt O_3 columns (Fig. S1 a et b, respectively). Note that the BASCOE simulations are driven by offline meteorological fields from ERA-Interim and performed after a 1 year spin-up with a horizontal resolution of 2.0°×2.5° and 60 levels in the vertical. Details on chemical mechanisms and parameterizations can be found in Huijnen et al., (2016) and Chabrillat et al. (2018). The purpose of this comparison is not to perform a proper validation/comparison exercise but to highlight and to estimate the "Jump" amplitude that affects the IASI MUSt O_3 time series and for which the exact reasons are still unknown. The "jump" in the IASI time series is clearly visible in the IASI-BASCOE difference panel on 15th September 2010 in the MUSt (see black arrow in Fig. S1a), while not in the LSt, as previously reported in the validation paper of Boynard et al. (2018). Based on that IASI-BASCOE comparison, the jump is estimated as reaching ~1-2 DU in the 55°S–55°N band and ~3-4 DU in the 55°–90° bands. These values are considered when analyzing trends in the MUSt O_3 time series in Sections 4.1 to 4.3 of the paper.

2 Figure S2

Figure S2 represents three typical examples of gridded daily time series of O_3 measured by IASI in the LSt over the period 2008-2017, after the natural variations fitted from MLR over the full IASI period have been removed. The significant fitted trends calculated over varying time periods from a single linear regression are superimposed. The trend values with associated uncertainties (within the 95% confidence level; in DU/yr) are indicated.

3 Figure S3

Figure S3 illustrates the time evolution of the lowest amplitude of the estimated trends in (a) total, (b) MUSt and (c) LSt O_3 columns over varying time periods that all end in December 2017, by subtracting the associated uncertainty (accounting for the autocorrelation in the noise residual; within the 95% confidence level) from the absolute value of the linear trends.

Figure caption

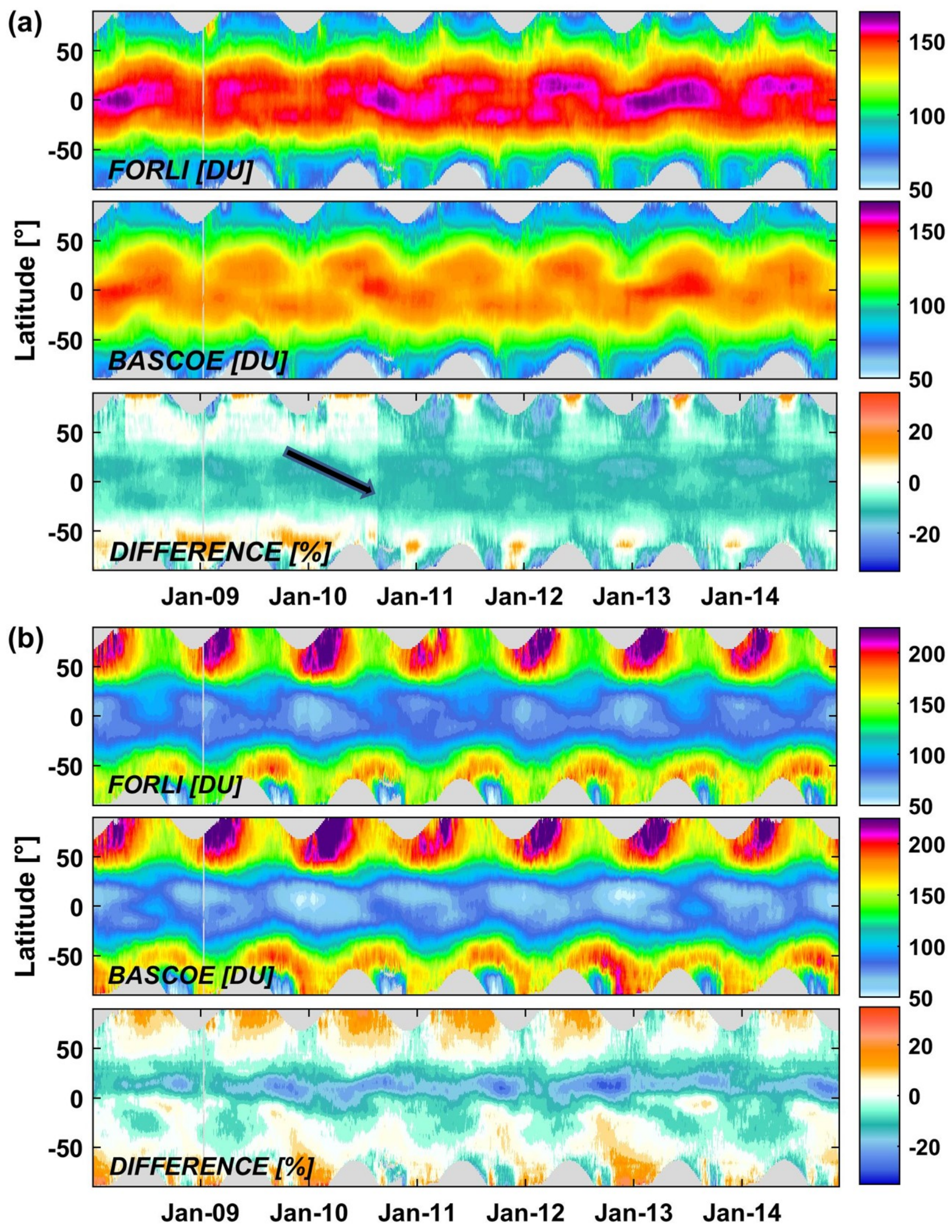

Fig. S1: Latitudinal distribution of (a) MUSt and (b) LSt O_3 columns as a function of time observed from IASI (in DU; top panels), simulated by BASCOE (in DU; middle panels) and of the IASI-BASCOE differences (in %; bottom panels). The black narrow in the difference panel for the MUSt highlights a jump on 15[th] September 2010.

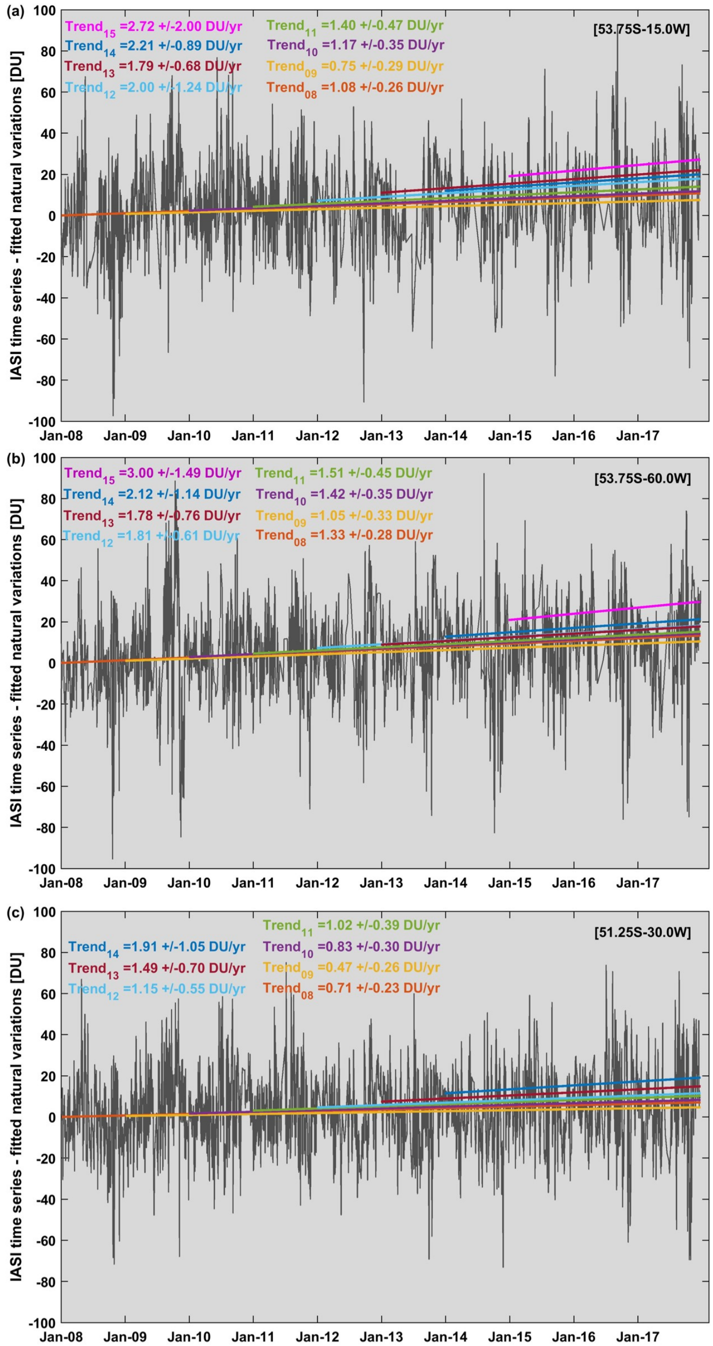

Fig. S2: Examples of gridded daily time series of O_3 measured by IASI in the LSt over the period 2008-2017 with all contributions to O_3 variations adjusted from MLR over the full IASI period removed, except for the trend (in DU). The significant fitted trends calculated over varying time periods from a single linear regression are superimposed. The trend values with associated uncertainties (within the 95% confidence level; in DU/yr) are indicated.

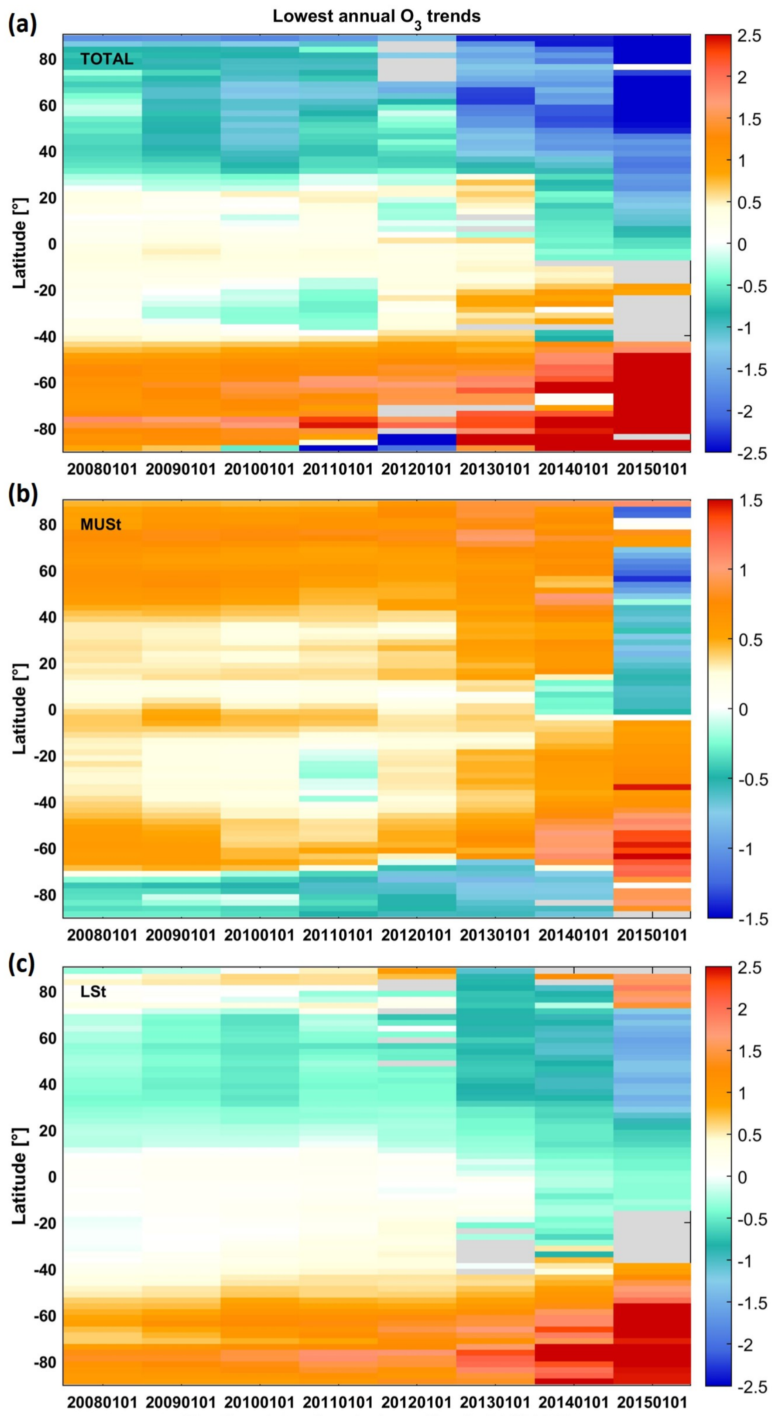

Fig. S3: Evolution of estimated linear trend minus the associated uncertainty accounting for the autocorrelation in the noise residual (DU/yr; within the 95% confidence level) in (a) the total, (b) the MUSt and (c) the LSt O_3 columns, as a function of the covered IASI measurement period ending in December 2017, with all natural contributions estimated over the full IASI period (2008-2017).